Nuclear-quadrupole-resonance measurement of the 27Al frozen core in YAlO3:Pr3+

Erickson, Lynden E.

Publisher's version / Version de l'éditeur:
https://doi.org/10.1103/PhysRevB.47.8734
Physical Review B, 47, 14, pp. 8734-8738, 1993-04

PHYSICAL REVIEW B VOLUME 47, NUMBER 14 1 APRIL 1993-II

Nuclear-quadrupole-resonance measurement of the ^{27}Al frozen core in $YAlO_3:Pr^{3+}$

Lynden E. Erickson
National Research Council, Ottawa, Ontario, Canada K1A 0R8
(Received 9 October 1992)

Nuclear-quadrupole-resonance measurements of four ^{27}Al frozen-core sites in $YAlO_3:Pr^{3+}$ in near-zero external static field are reported. The measurements were made by observing the effect of a weak radio-frequency magnetic field resonant with the ^{27}Al nucleus on the ^{141}Pr nuclear-quadrupole echo. The echoes were detected optically using a Raman heterodyne method. Most of the resonance lines show a doubling that is attributed to a magnetic field produced by the $^{141}Pr^{3+}$ enhanced nuclear moment as the doublet separation is dependent on the nuclear sublevels of the $^{141}Pr^{3+}$ ion used in the measurement.

I. INTRODUCTION

In experiments studying the coherence dephasing of ions in optical solids, the strong role played by nuclear moments of host nuclei has been noted.[1,2] This has been illustrated by Yano, Mitsunaga, and Uesugi[3] by employing a Y_2SiO_5 host, in which the only nuclear moment is the 4.7% abundant ^{29}Si, in a photon echo experiment. Dephasing times as long as 800 μs were observed. The host nuclei act as two different dephasing agents. Those far removed from the paramagnetic guest ion undergo rapid mutual spin flips with other host nuclei as they are all resonant with one another. This produces a small-amplitude high-rate magnetic field modulation at the guest ion, which is responsible for the two-pulse echo decay for times exceeding a few tenths T_2. The near-neighbor host nuclei are influenced by the guest paramagnetic ions which detune them from the bulk nuclei, so they undergo slow mutual spin flips with only resonant near neighbors. The result is a low-rate large-amplitude modulated magnetic field at the guest ion. The three-pulse stimulated echo decay is dominated by these frozen-core spin flips.[4,5] Spin flips of Al nuclei dephase the Pr nuclear-quadrupole echoes by detuning the Pr resonance frequences. External radio-frequency (rf) magnetic fields inducing magnetic dipole transitions of Al also dephase the Pr echoes. In this paper, measurements of the ^{27}Al nuclear-quadrupole-resonance (NQR) spectrum, detected by the effect of ^{27}Al magnetic dipole transitions on the two-pulse NQR ^{141}Pr echo, in the host crystal $YAlO_3$ are reported. $YAlO_3$ is also known as yttrium aluminum perovskite or YAP.

Burum, Macfarlane, and Shelby[6] (BMS) measured the NQR spectra of ^{27}Al in $YAlO_3:Pr^{3+}$ using a two-pulse photon echo detection method and compared those results with the bulk ^{27}Al zero-field splittings extrapolated from their high-field nuclear-magnetic-resonance (NMR) measurements[7] at higher temperatures. From their measurements, they concluded that the frozen-core detuning was largely due to changes in the electric-field gradients caused by substitution of the paramagnetic Pr^{3+} guest ion. This conclusion is consistent with the expectation that there is no permanent magnetic moment for the non-degenerate electronic ground state of Pr^{3+} in the absence of an external magnetic field. But the Pr nuclear moment produces an electronic moment in the Pr^{3+} ion. This combined Pr moment produces a magnetic field at the near-neighbor Al nuclei which detunes the resonant frequencies of neighboring nuclei from those nuclei which are farther away from the paramagnetic moment. Magnetic detuning must be responsible for the frozen core observed[8] in $LaF_3:Pr^{3+}$. The nuclear spin of fluorine is 1/2; there is no nuclear-quadrupole zero-field splitting. Is the absence of a magnetic detuning in $YAlO_3:Pr^{3+}$ only a fortuitous cancellation? The results of this paper show evidence that the hyperfine induced magnetic moment of Pr^{3+} exerts a field of as much as 10 G on the neighboring Al nuclei in the absence of an external static field and that the Al zero-field NQR frequencies are dependent on the nuclear sublevel of the nearby Pr^{3+} ion as well as on the site of the Al nuclei.[9]

II. EXPERIMENT

An early NQR double-resonance measurement in a solid was made by Emshwiller, Hahn, and Kaplan.[10] They applied a π pulse to the unknown (B) spin during the π pulse of a two-pulse nuclear-spin echo sequence for a known spin (A) and observed the resonance by a reduction of the A-spin-echo amplitude. The experiment of this paper differs from theirs in that a much weaker B-spin rf magnetic field is applied during the entire time from the end of the first A-spin pulse to just before the echo, and by use of Raman heterodyne detection[11] of the Pr^{3+} nuclear-quadrupole echo in this dilute material. In essence, it replaces the photon echo detection scheme of BMS with a NQR detection method.

The measurements were made as previously reported.[4] The $YAlO_3:Pr^{3+}$ (0.05 at. %) single crystal, mounted in a delay line coil[12] in a cryostat at approximately 5.5 K, was illuminated by a 16 874.7 cm^{-1} 50 mW beam from a frequency-stabilized dye laser for a 36 ms period to polarize the ^{141}Pr nuclei. After a 7 ms dark period to ensure that the 0.5 ms lifetime excited $^1D_2$ (16 874.7 cm^{-1}) state was unpopulated, the rf pulse sequence was applied to the sample in the dark. The first rf (^{141}Pr NQR frequency $=\nu_1$) pulse was 5.7 μs long and the separation between its center and the center of the 11.4 μs second (ν_1) pulse was

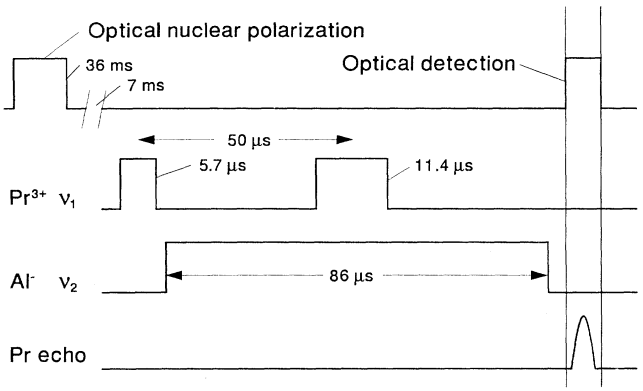

FIG. 1. This pulse sequence was used to measure the Al NQR by observing the effect of the Al rf magnetic field (ν_2) on the Pr nuclear-quadrupole echo. The first optical pulse polarizes the Pr nuclei by optically pumping the ground-state hyperfine levels via the $^1D_2$ (16 374.7 cm^{-1}) optical transition. After a 7 ms dark period to allow the 0.5 ms lifetime excited state to decay,the two-pulse Pr rf sequence (ν_1) is applied to the sample. The weak Al rf pulse is applied between the end of the first Pr pulse and the expected time of the echo. At the expected time of the echo, the optical pulse is turned on to observe the echo.

50 μs (Fig. 1). The peak rf magnetic field generated by these pulses was about 25 G. A second rf (^{27}Al NQR frequency $=\nu_2$) magnetic field ($\approx$2 G) was applied to the sample beginning after the 5.7 μs pulse and ended just prior to the echo; it was 86 μs in duration. The echo was observed using Raman heterodyne detection[9] by illuminating the crystal with the laser beam at the time of the echo. The light which passed through the crystal illuminated a photodiode. Its amplified signal was connected to a balanced mixer (local oscillator frequency $=\nu_1$) and a digital oscilloscope. Two acousto-optic (AO) modulators were used to switch the light beam. A set of measurements was made by fixing ν_1 at the ground-state $^{141}Pr^{3+}$ $I_z=3/2\leftrightarrow I_z=5/2$ transition near 14.1 MHz (Ref. 13) and by varying the second ^{27}Al rf frequency ν_2 from 280 to 1100 kHz in steps of 2.5 or 5 kHz after each pulse sequence. Another set of measurements was made by fixing ν_1 at the ground-state $^{141}Pr^{3+}$ $I_z=1/2\leftrightarrow I_z=3/2$ transition near 7.07 MHz. Typically, 32 echoes were averaged for each ^{27}Al frequency. The pulses were repeated at 1 s intervals. The laser frequency was slowly swept (200 MHz in 6 s) to avoid saturating the echo signal.

III. RESULTS

Typical results are shown for near-zero static external magnetic field in Fig. 2, and for a static external magnetic field of 10 G along the b axis in Fig. 3. In zero field and for a magnetic field along the b axis, the two Pr^{3+} sites are magnetically equivalent. The observed ^{27}Al peaks for the Al nuclei in the vicinity of either Pr site fall at the same frequencies.[14] With static magnetic fields at more general angles, the ^{27}Al resonances for the two Pr sites are distinct, and can be selectively observed depending on which Pr site is excited by the two-pulse sequence. For the low-frequency measurements (from 280 to 650 kHz) the Al rf magnetic-field amplitude was about one-third of that required for the high-frequency measurements (from 700 to 1100 kHz). No peaks were observed between 1100 and 1800 kHz. The amplitude of the observed peaks increased linearly as the rf magnetic field was varied near the rf level used for Fig. 2. A further increase by a factor 2 led to a weak nonlinear increase for the level at 455 kHz, and weaker nonlinear responses from several other lines. Amplitude noise in the spectra makes quantitative conclusions about the nonlinearity difficult. The transition at 455 kHz may consist of two components: one is a transition between two real levels, and the other is a two-quantum transition connecting 322 and 590 kHz (Ref. 6) or a second harmonic transition at 910 kHz. Weak rf B-spin magnetic fields were used to avoid the complication of these multiple quantum transitions. The $I_z=1/2\leftrightarrow I_z=3/2$ zero-field frequency of the *excited* $^{141}Pr^{3+}$ $^1D_2$(16 874.7 cm^{-1}) level at 920 kHz (Ref. 15) would fall in the midst of the frequency data, but the 7 ms delay after the optical polarizing pulse allows this 0.5 ms lifetime state to fully decay before applying the two-pulse sequence. This ensures that the excited-state transition is *not* observed. It is further confirmed by the absence of the $I_z=3/2\leftrightarrow I_z=5/2$ zero-field frequency transition at 1567 kHz.

The most striking characteristic of the data in Fig. 2 is the doubling of the zero-field peaks compared with broader single peaks observed by BMS. There appear to be four doublets in the low-frequency group (322, 363; 435, 456; 495, 530; and 573, 593), and three doublets in the high-frequency group (769, 819; 905, 946; and 946, 972) for the Pr $I_z=3/2\leftrightarrow I_z=5/2$ echo detection[Fig. 2(b)]. And for the Pr $I_z=1/2\leftrightarrow I_z=3/2$ echo detection, one doublet in the low-frequency group at 335 and 354 kHz, and two single levels at 447 and 515 kHz are observed [Fig. 2(a)]. The high-frequency group for the Pr $I_z=1/2\leftrightarrow I_z=3/2$ echo detection consists of doublets at 778 and 814 kHz, 905 and 945 kHz, and a single level at 959 kHz. The observed linewidths vary from 12 to 17 kHz full width at half maximum (FWHM). For a B-spin pulse duration of 86 μs, the experimental resolution is about $1/(\pi 8.6\times 10^{-5})$ or $\approx$4 kHz. The low-frequency group consists of the $S_z=1/2\leftrightarrow S_z=3/2$ and $S_z=3/2\leftrightarrow S_z=5/2$ transitions of the ^{27}Al nuclei for several sites.[16] The upper frequency group are the lower transition probability $S_z=1/2\leftrightarrow S_z=5/2$ ^{27}Al transitions. The doubling of the zero-field lines is only a function of which Pr NQR transition is used for detection, and is independent of rf magnetic-field amplitudes, pulse spacings, and duration of the pulses. The measured Al linewidth does change as the Al NQR pulse duration changes, with the product of the linewidth and the pulse width approximately 1.

These data should be compared with the BMS photon echo detected Al NQR. They reported data up to about 700 kHz. They observed ^{27}Al transitions at 340, 450, 520, and 580 kHz. From their high-field NMR data,[17] they conclude that bulk Al frequencies are 341 and 455 kHz which would give a $S_z=1/2\leftrightarrow S_z=5/2$ transition at

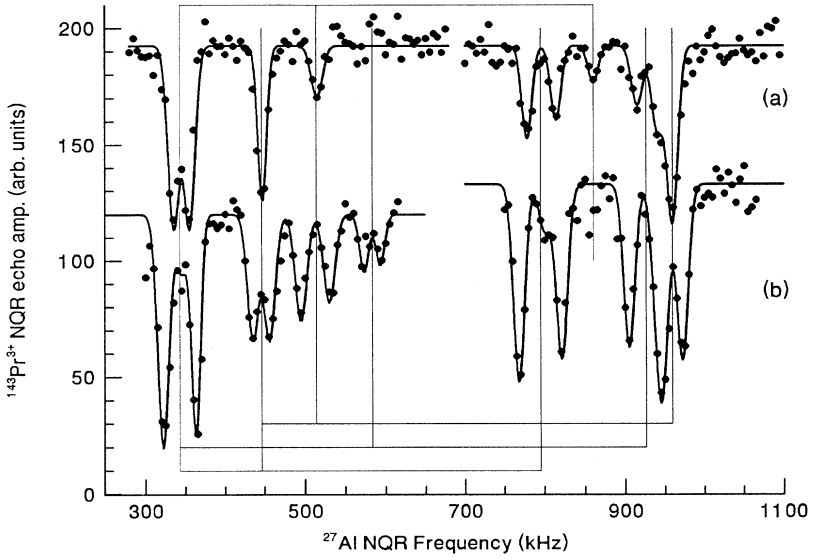

FIG. 2. The near-zero-field ^{27}Al NQR spectra are shown when (a) observed via the Pr^{3+} NQR $I_z=1/2\leftrightarrow I_z=3/2$ transition and (b) via the Pr^{3+} NQR $I_z=3/2\leftrightarrow I_z=5/2$ transition. The upper trace has been offset for clarity. The external magnetic field was 2 G along the b axis of the crystal for (a) and less than 1 G for (b). A small magnetic field is needed to observe the Pr NQR echoes with this Raman heterodyne optical detection method.

796 kHz. At these frequencies, a weak peak at 345 kHz is observed between a pair of strong lines in our Pr $I_z=3/2\leftrightarrow I_z=5/2$ NQR echo data, together with a peak at 456 kHz. They also conclude that the only ^{27}Al frozen-core peaks are at 340 and 580 kHz and by extension, a high-frequency peak at 920 kHz. In this experiment, each of those peaks is split into pairs separated by 41, 20, and 20 kHz, respectively. In addition, they identify a peak at 455 kHz as a double quantum peak by its dependence on rf power.

The mean frequency of the doublets and single lines is independent of the Pr detecting transition. The mean transition frequencies for both Pr NQR echo frequencies ν_1 are listed in Table I. It is possible to identify four sites from these mean frequencies. The lines identified by BMS as bulk lines at 342, 455, and 796 kHz are labeled as site I. Transitions are observed at all three frequencies. Other lines are observed for frozen-core sites and are labeled as site II through site IV. BMS observed two frozen-core sites for Eu^{3+} in $YAlO_3$ but only one for Pr which we label site II. The presence of the four $S_z=1/2\leftrightarrow S_z=5/2$ transitions indicates four frozen-core sites for each Pr site. These may be fitted by a quadrupolar Hamiltonian

$$H=P\left[\left[S_z^2-\frac{1}{3}S^2\right]+\frac{\eta}{3}(S_x^3-S_y^2)\right] \tag{1}$$

to obtain the parameters listed in Table I. Here S is the nuclear spin of Al, $P=3e^2qQ/40$ is the quadrupole coupling constant, and η is the asymmetry parameter. The quadrupolar constant P, all in a narrow band from 120 to 150 kHz, show that the field gradients seen by all of the Al nuclei are quite similar. The asymmetry differs significantly from site to site. The largest asymmetry is at site III, where $P=141.2$ kHz and $\eta=0.833$; the asymmetry parameter η is slightly larger than that for one of the Eu^{3+} sites in the same host.[6] Normally, one would expect only two frozen-core sites. The Al have two distinct sites in the bulk whose quadrupolar axes are not aligned with the quadrupolar axes of the two Pr sites. In the absence of a field, or with a small bias field along one

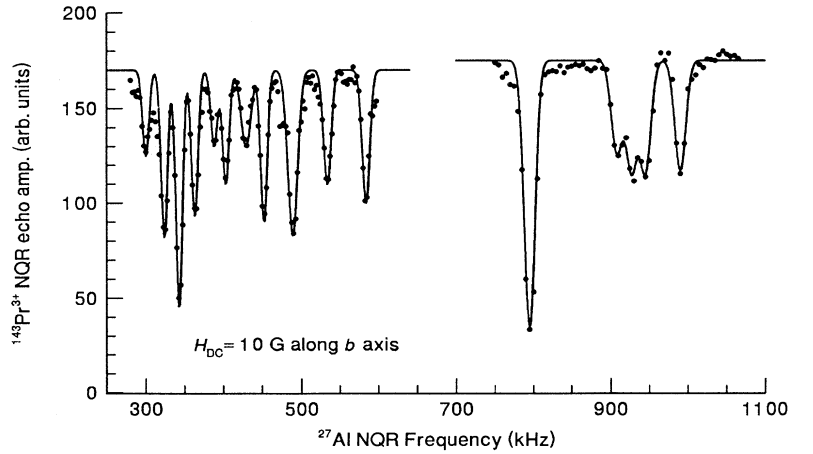

FIG. 3. The ^{27}Al NQR spectra are shown when observed via the Pr^{3+} NQR $I_z=3/2\leftrightarrow I_z=5/2$ transition with an external magnetic field of 10 G along the b axis of the crystal.

TABLE I. The mean of the near zero-field ^{27}Al NQR doublets and their pure quadrupole parameters P and η is given in this table. The site BMS identified as bulk Al (Refs. 6 and 12) is labeled as site I. The sum of the first two frequencies is given in parentheses in the second column.

Site	Mean frequencies (kHz)	P (kHz)	η
I	342, 445, 794 (787)[a]	120.0	0.6934
	344, 447, 796 (791)[b]		
II	342, 583, 925 (925)[a]	149.6	0.3752
	344, 927[b]		
III	445, 512, 959 (957)[a]	141.2	0.8333
	447, 525, 959 (962)[b]		
IV	344, 515, 860 (859)[b]	135.2	0.5344

[a]Measurement made using the $I_z=3/2\leftrightarrow I_z=5/2$ $^{141}Pr^{3+}$ NQR transition.
[b]Measurement made using the $I_z=1/2\leftrightarrow I_z=3/2$ $^{141}Pr^{3+}$ NQR transition.

of the crystal axes, the bulk Al are equivalent. The near neighbors will be perturbed by the Pr^{3+} ion which will remove that equivalence. The third and fourth sites may be due to the next nearest neighbors of a Pr^{3+} ion.

These measurements show that the doubling (splitting) of the zero-field quadrupole levels is related to the Pr nuclear levels occupied by the detecting Pr^{3+} ion. If the splitting is due to the Pr^{3+} electronic moment, one would not expect the bulk Al which are far away from the enhanced Pr moment to be split because the local field falls off as r^{-3} where r is the Al-Pr internuclear distance. The photon echo measurement (BMS) would show no splitting because the measurement includes a sum of all possible Pr levels, both ground and excited states. A number of possible models were examined. (a) Pake[18] observed a splitting of this form for the protons in $CaSO_4 \cdot 2H_2O$. The splitting of 22 G maximum was due to the magnetic dipole interaction of the two protons bound to the oxygen in the water of hydration. The H↔H distance was 1.58 Å compared to 3.70 Å for the nearest Al↔Al and the nuclear moments are 2.79 and 3.64 nm, respectively. Because of the cubic dependence on internuclear distance, the maximum Al-Al splitting in $YAlO_3$ would be about 2 G for both Al in the $I_z=5/2$ sublevel. (b) Another model was given by Teplov for concentrated materials.[19] In his experiments on TmF_3, he found that the dipolar Hamiltonian was unable to predict the energy levels; an exchange and an indirect (electron mediated) J-coupling term was required to fit the data. Values as high as 40 kHz were observed, largely due to exchange of Tm-F, Tm-F. While exchange for a dilute material is excluded, the enhancement of the Pr nuclear moment is similar in this J coupling. Both are indistinguishable experimentally from the direct dipole-dipole coupling. The most likely model is one where the Al nuclei are exposed to the Pr hyperfine enhanced dipole moment and the observed splitting is a result of the state of the Pr^{3+} ion during the measurement period. Sharma and Erickson[20] used such a model in examining the coupled Pr-F NQR spectra of $LiYF_4$:Pr^{3+}, where the Pr system has a spin 5/2 and the F system has a nuclear spin 1/2 . A Hamiltonian, including a dipolar part for the spin 1/2, spin 5/2 systems, the quadrupole part for Pr, and the Zeeman terms for both Pr and F, was used. The Pr-Al system is even more complex. And since we are using Pr nuclear-spin echoes in our measurement, the Al nucleus will experience the field of a *superposition* Pr nuclear state during the time of the B-spin rf field, either $\langle I_z \rangle=(1/2+3/2)/2$ or $\langle I_z \rangle=(3/2+5/2)/2$. This superposition state would have to be accounted for in the theoretical treatment.

The magnetic-field ($\propto \langle I_z \rangle$) ratios between the measurements made for $I_z=1/2\leftrightarrow I_z=3/2$ and $I_z=3/2\leftrightarrow I_z=5/2$ is 1:2. The doublet centered at 345 kHz shows a ratio of 19:41. Other doublets centered at 925 and 959 kHz shows ratios near 1:1.5. The bulk Al nuclei must be farther away from the Pr^{3+} ion and should show little or no doubling. The bulk Al levels chosen by BMS show doubling of 41, 21, and 50 kHz for $\langle I_z \rangle=2$ and 19, 0, and 36 for $\langle I_z \rangle=1$, but buried within the 322 and 363 kHz doublet is a peak at 345 kHz. The doublet centered at 455 kHz peak is insufficiently resolved to recognize a central peak if any. Site III shows no doubling for $\langle I_z \rangle=1$ but the doubling is 20, 35, and 30 kHz for $\langle I_z \rangle=2$. As was pointed out by Sharma[20] in his perturbation treatment of Pr-F, for fields less than about 5 G, this simple approach does not correspond with reality. A complete mathematical model is required to understand this behavior, but such an analysis is beyond the scope of this paper.

The large splitting of the ^{27}Al levels identified by BMS as bulk sites (and in this work as site I) is troubling. One must conclude that a doubled resonance is not from a bulk Al site. A direct zero-field NQR of bulk Al at helium temperatures would enable a clearer identification of the bulk sites than the extrapolation to zero field and low-temperature use by BMS. Usually some paramagnetic species are required in the crystal to prevent saturation of the NQR signals and as we have seen, the Al nuclei which are relaxed are also perturbed. The measurement would likely have to be made in an undoped material to exclude Al immediately surrounding the frozen core of the paramagnetic ion. Those in the frozen core probably will not contribute because of their small numbers and because of their long dephasing times.

Application of a 10 G static magnetic field splits these transitions except for the 795 kHz for which an accidental crossing of the 769 and 819 kHz zero-field resonances occurs. The strong zero-field resonances at 323 and 365 kHz become five at 300, 324, 343, 363, and 388 kHz in

the 10 G field with the lines becoming sharper (8 kHz). Other resonances are observed at 403, 429, 452, 474, 490, 534, 584, 795, 908, 927, 945, and 990 kHz. The signals are much stronger in a magnetic field because the magnetic field removes a zero-field symmetry cancellation of the Raman heterodyne Pr^{3+} echo.[21] One observes changes in frequency of 20 to 27 kHz for a 10 G change in field instead of the bare Al nucleus value of 10 kHz. This enhancement indicates that the presence of the nearby paramagnetic Pr ion is important. For larger fields (up to the 80 G limit of the magnet), the high density of lines makes interpretation very difficult. As noted above, one can simplify the data by identifying the spectra of Al nuclei in the vicinity of a specific Pr site by tuning ν_1 to a frequency of one of the two Pr sites when the external magnetic direction is not along a crystal axis. It would be desirable to have a full magnetic-field rotation spectrum so that a complete analysis of the system could be made. Some data were obtained, but not enough for full rotation studies of the Al NQR. In view of the long measurement times required for each field direction, this was not completed.

IV. CONCLUSIONS

The NQR spectrum of Al which are near neighbors of Pr in $YAlO_3$:Pr^{3+} has been observed, including resonances from four Al sites. A large splitting of each zero-field NQR transition is attributed to the magnetic field produced by the enhanced nuclear moment of the nearby Pr^{3+} ion. This field is a function of the nuclear-spin state of the Pr^{3+} ion, as the observed doubling was a function of the Pr transition used to detect the Al NQR. When a 10 G magnetic field is applied to the sample, the NQR spectra become complex. The association of the Al site with a particular Pr^{3+} was made in a small static external magnetic field, when the NQR resonances of the two Pr sites were resolved, by detecting Al NQR on a particular Pr^{3+} transitions.

ACKNOWLEDGMENTS

I wish to thank A. Szabo for many useful discussions during the course of this work, N. B. Manson for communicating his results prior to publication, and J. Froemel for technical assistance.

[1]R. M. Macfarlane, R. M. Shelby, and R. L. Shoemaker, Phys. Rev. Lett. **43**, 1726 (1979); P. Hu and S. R. Hartmann, Phys. Rev. B **9**, 1 (1974).

[2]R. G. DeVoe, A. Wokaun, S. C. Rand, and R. G. Brewer, Phys. Rev. B **23**, 3125 (1981).

[3]R. Yano, M. Mitsunaga, and N. Uesugi, Opt. Lett. **16**, 1884 (1991).

[4]L. E. Erickson, Phys. Rev. B **43**, 12723 (1991).

[5]Y. S. Bai and R. Kachru, Phys. Rev. A **44**, R6990 (1991).

[6]D. P. Burum, R. M. Macfarlane, and R. M. Shelby, Phys. Lett. A **90**, 483 (1982).

[7]D. P. Burum, R. M. Macfarlane, R. M. Shelby, and L. Mueller, Phys. Lett. A **91**, 465 (1982).

[8]L. L. Wald, E. L. Hahn, and M. Lukac, J. Opt. Soc. Am. B **9**, 789 (1992).

[9]A similar result for Ho^{3+} has been reported by J. P. D. Martin, T. Boonyarith, N. B. Manson, and Z. Hasan, J. Phys. Condens. Matter **4**, L411 (1992).

[10]M. Emshwiller, E. L. Hahn, and D. Kaplan, Phys. Rev. **118**, 414 (1960).

[11]J. Mlynek, N. C. Wong, R. G. DeVoe, and R. G. Brewer, Phys. Rev. Lett. **50**, 993 (1983).

[12]I. J. Lowe and M. Engelsberg, Rev. Sci. Instrum. **45**, 631 (1974).

[13]L. E. Erickson, Phys. Rev. B **19**, 4412 (1979); **24**, 5388 (1981).

[14]There is only one naturally occurring isotope for Y, Al, and Pr. The only isotope "impurities" are ^{17}O (0.037%) and ^{18}O (0.20%).

[15]Y. S. Bai and R. Kachru, Phys. Rev. Lett. **67**, 1859 (1991); M. Mitsunaga, R. Yano, and N. Uesugi, Phys. Rev. B **45**, 12 760 (1992).

[16]The angular momentum of nuclear spins are labeled as I for the Pr rare nuclei and S for Al abundant nuclei. The Pr^{3+} electronic angular momentum will be labeled J.

[17]D. P. Burum, R. M. Macfarlane, and R. M. Shelby, Phys. Lett. **91A**, 465 (1982).

[18]G. E. Pake, J. Chem. Phys. **16**, 327 (1948).

[19]M. V. Eremin, I. S. Konov, and M. A. Teplov, Zh. Eksp. Teor. Fiz. **73**, 569 (1977) [Sov. Phys. JETP **47**, 297 (1977)].

[20]K. K. Sharma and L. E. Erickson, J. Phys. C **14**, 1329 (1981).

[21]Thus the need to have a small bias field present for the zero-field measurements of Fig. 2.